Combined X-ray and neutron single-crystal diffraction in diamond anvil cells

Andrzej Grzechnik [1,*], Martin Meven [1,2], Carsten Paulmann [3], Karen Friese [4]

[1] Institute of Crystallography, RWTH Aachen University, 52056 Aachen, Germany
[2] Jülich Centre for Neutron Science (JCNS), Forschungszentrum Jülich GmbH at Heinz Maier-Leibnitz Zentrum (MLZ), 85748 Garching, Germany
[3] Mineralogisch-Petrographisches Institut, Universität Hamburg, 20146 Hamburg, Germany
[4] Jülich Centre for Neutron Science-2 / Peter Grünberg Institut-4 (JCNS-2/PGI-4), Forschungszentrum Jülich GmbH, 52425 Jülich, Germany

[*] Corresponding author: grzechnik@xtal.rwth-aachen.de

Abstract

It is shown that it is possible to perform combined X-ray and neutron single-crystal studies in the same diamond anvil cell (DAC). A modified Merrill-Bassett DAC equipped with an inflatable membrane filled with He gas was developed. It can be used on laboratory X-ray and synchrotron diffractometers as well as on neutron instruments. The data processing procedures and a joint structural refinement of the high-pressure synchrotron and neutron single-crystal data are presented and discussed for the very first time.

Introduction

X-ray and neutron diffraction are complimentary experimental techniques for detailed studies of crystalline materials. Neutron diffraction is indispensable when X-ray diffraction fails to probe, for instance, magnetic (dis)order (Devi *et al*., 2019), compounds containing light elements (Truong *et al*., 2018), or (dis)ordering of elements over crystallographic sites (Hering *et al*., 2015). Due to the complementarity of X-ray and neutron data, their joint use allows to study compounds, in which magnetic order has a direct influence on the underlying crystal structure or vice versa, e.g., magnetocalorics (Hering *et al*., 2015). In experimental electron density studies of molecular crystals, combined X-ray and neutron single-crystal diffraction is frequent and often mandatory to fully understand the nature of bonding (Jarzembska *et al*., 2017). The capabilities of neutron scattering at extreme conditions have been reviewed by Guthrie (2015).

Owing to the tremendous development of radiation sources and area-sensitive detectors, single-crystal X-ray diffraction in a diamond anvil cell (DAC) can now be performed on very small samples ($< 10^{-7}$ mm^3) with complex crystal structures up to megabar pressures (Merlini & Hanfland, 2013). On the other hand, there are only two single-crystal neutron diffraction studies in DAC with complete structural refinements (Binns *et al*, 2016; Grzechnik *et al*., 2018). The reason for this is that even at the most advanced neutron facilities it is difficult to study crystals with volumes below 1 mm^3 since the highest neutron fluxes are several orders of magnitude smaller than the photon fluxes at synchrotron sources. Single crystals of several cubic millimetres are routinely studied with neutron scattering using gas-pressure and clamp cells (Klotz, 2013; Ridley & Kamenev, 2014). Data collected in Paris-Edinburgh presses are suitable for structure refinements at short neutron wavelengths (Bull *et al*., 2011) but are very restricted in reciprocal space. The *panoramic* cells with big anvils made of sapphire (Kuhs *et al*., 1989, 1996; McMahon *et al*., 1990) or moissanite (McIntyre *et al*., 2005) have been used to collect data for full structure

refinements but cannot be used for X-ray diffraction experiments (no transmission through gasket). The requirement for large samples in neutron scattering hinders the joint use of X-ray and neutron single-crystal diffraction upon compression. Up to now, no complimentary crystallographic studies at high pressures on exactly the same sample under exactly the same experimental conditions have been performed. In addition, diamond anvil cells that are suitable both for X-rays and neutron diffraction studies are not commonly available.

Recently, we have started exploring the feasibility of neutron measurements in DAC on the four-circle single-crystal diffractometer HEiDi (Meven & Sazonov, 2015) at the Heinz Maier-Leibnitz Zentrum (MLZ) in Garching. Using the hot source of the FRM II reactor, HEiDi operates at short monochromatic wavelengths with high fluxes. It is equipped with a point detector (Eurisys, 5 bar ^{3}He) with a high sensitivity (>95%) down to λ = 0.3 Å. It provides precise information on crystal and magnetic structures, including the reliable and accurate characterisation of anisotropic displacement parameters (ADP) in materials with highly absorbing elements. Typical investigations at HEiDi focus on [1] ionic conductors relevant for energy applications and data storage (Ceretti *et al*., 2018), [2] superconductors (Jin *et al*., 2016), [3] multiferroic materials (Regnat *et al*., 2018), [4] small-molecule structures, in which hydrogen bridges play a key role as a structure building element (Truong *et al*., 2017, 2018), or [5] complex zeolitic crystal structures (Gatta *et al*., 2018).

For our high-pressure work at HEiDi, we constructed a *panoramic* diamond anvil cell with large access to reciprocal space (Grzechnik *et al*., 2018). The data measured using this cell have a completeness of 76% (θ_{full} = 39.34 °, λ = 1.17 Å) and are of excellent quality, as demonstrated by a full structure refinement with standard tools in high-pressure crystallography (Friese *et al*., 2013; Petricek *et al*., 2014). This cell is also compatible with the cryostats available at MLZ (Eich *et al*., 2019). However, *panoramic* cells, in which both incident and diffracted beams pass through the gasket, cannot be used for combined X-ray and neutron diffraction studies, because there is no

gasket material that weakly attenuates neutrons and at the same time is transparent to high-energy X-ray radiation. Hence, cells working in the *transmission* mode are optimal for such experiments as the incident and diffracted beams pass through the diamond anvils, which only weakly attenuate both X-rays and neutrons. The first cells for combined X-ray and neutron studies were developed by Goncharenko (Goncharenko, 2007). They are called *hybrid* DAC since they have windows for *panoramic* (neutron) and *transmission* (X-ray) geometries. However, these windows only allow to measure the data at very small scattering angles due to their limited opening angles. Consequently, comprehensive structural refinements are possible neither from the neutron nor from the X-ray data obtained in the *hybrid* DAC due to the insufficient number of accessible reflections.

Here, we present *transmission* cells suitable for both neutron and X-ray single-crystal diffraction with a comparatively large opening angle of 80°. They can be used on various diffractometers at laboratory X-ray, synchrotron and neutron facilities. The joint structural refinement of a crystal structure from the neutron and synchrotron data at high pressures measured under identical conditions is performed and discussed here for the very first time.

For our combined benchmark X-ray and neutron measurements, we chose a crystal of $MnFe_4Si_3$ that was already investigated in our earlier high-pressure neutron single-crystal diffraction study (Grzechnik *et.al*., 2018). The structure of this compound is well known and was determined at ambient conditions using joint X-ray and neutron data (Hering *et al*., 2015). While the atomic coordinates can be straightforwardly obtained from X-ray diffraction, the occupation factors for the mixed occupancy site incorporating Mn and Fe (i.e., neighbouring elements in the periodic table) can only be determined from neutron diffraction since the two elements have largely different scattering lengths.

The cells

The design of our *transmission* cells is a modification of the generic DAC type with a three-fold symmetry by Merrill and Bassett (1974). They are cylindric with the central part having a four-fold symmetry and fitted with conical diamonds (type Ia, aperture 80°). The angular opening angle is 80°. The four guiding pins are integrated in the body of the cell. The smallest cell is 30 mm in diameter and 20 mm in height. Pressure is generated by tightening four M3 bolts. A larger cell, with 44 mm in diameter and 25 mm in height (Figure 1a), is equipped with a remotely inflatable membrane filled with He gas (memDAC). The diamonds can be aligned both in a parallel and translational manner. Pressure in this cell is generated by tightening four M4 bolts and/or by inflating the membrane (LeToullec *et al*., 1992; Goncharenko, 2007). A valve attached to the membrane through a capillary allows disconnecting the cell from a pressure controller, while maintaining the pressure in the membrane. The size of the outside membrane cup is 50 mm in diameter and 33 mm in height. The outer dimensions of both cells and of the membrane cup are quite small so that the same crystal could be studied at the same conditions on laboratory X-ray and synchrotron diffractometers as well as on neutron beamlines (Figures 1b and 1c). Our memDAC is especially useful to follow the pressure dependence of selected reflections by using the remotely inflatable membrane. The use of the membrane avoids safety concerns related to tightening the screws by hand when the sample might be activated by the exposition to the neutron beam. The small size of the cells also makes them suitable for low-temperature investigations in closed-cycle cryostats when the membrane is not used.

All parts of the cells, except for the diamonds (https://diamondanvils.com/) as well as the membrane, capillary, and valve (all three from http://betsa.fr/), are currently made of Berylco-25 (CuBe). The pressures reachable with diamonds culets of 0.6 mm and 1.0 mm in diameter are above 10 GPa and 4 GPa, respectively. Alternatively, the M3 and M4 bolts can be made of high tensile titanium alloys (Klotz, 2013). DAC could also be produced from the Ni-Cr-Al alloy ("*Russian alloy*", NiCrAl) with superior mechanical properties to CuBe (Cheng *et al*., 2019).

Unlike most of the materials that are used to manufacture DAC for X-ray diffraction, CuBe and NiCrAl are ideal both for X-ray and neutron diffraction as they are non-magnetic down to very low temperatures and weakly attenuate neutrons. Our memDAC made of CuBe does become activated by neutrons but always remains below the safety limits for free handling. In contrast, the most common maraging steels are not paramagnetic and become highly activated with neutrons due to a significant content of cobalt.

Data collection and processing

An approximately prismatic crystal of $MnFe_4Si_3$ (about 0.4*0.45*0.6 mm^3) was loaded into memDAC together with a ruby chip. The size of the crystal is only slightly larger than the minimal one for the crystals that currently can be measured at HEiDi (Grzechnik *et al*., 2018). The diameter of the diamond culets was 1.5 mm. To load such a large crystal and avoid crushing it between the anvils, the gasket with an initial thickness of 1 mm was pre-indented to about 0.8 mm. The initial diameter of the sample chamber was 0.8 mm. With so thick a pre-indentation, the pressure is limited by the stability of the gasket. We therefore performed our benchmark measurement at a fairly low pressure of 0.9 GPa to ensure a stable pressure for both the neutron and synchrotron measurement, despite the fact that the pressure limits for the cell are higher (see above).

To minimize the background due to neutron scattering from all the components of the cell, the conical surfaces of the seats as well as of both upper and lower parts of the cell were covered with a gadolinium paint, i.e., a fine powder of Gd_2O_3 mixed with a nail polish (see the white paint on the cell in Figures 1b and 1c). As a result, the holes in the seats effectively acted as pinholes with the diameter of 3.2 mm, i.e., the diameter of the diamond table. The pressure determined using ruby luminescence was 0.9 GPa. The transmitting medium was a deuterated 4:1 mixture of methanol and ethanol.

Prior to the neutron measurements on HEiDi, we determined the orientation matrix of the crystal in DAC on the laboratory single-crystal STOE diffractometer IPDS-II (Mo-Kα) (Figures 1b and 1c). The collected data were processed with the software X-Area (Stoe & Cie, 2013).

Unlike in the original Merrill-Bassett type (Merrill & Bassett, 1974; Binns *et al.*, 2016), the use of the membrane precludes the neutron data collection through the cell body of our DAC. Hence, the diffracted neutron intensities (Table 1) were measured within the cones of the cell (the opening angle 80°). The HEiDi diffractometer has a four-circle Eulerian geometry. At the beginning of the neutron experiment (λ = 1.17 Å), memDAC was oriented with its axis coinciding with the primary beam, i.e., all diffractometer axes 2θ, ω, χ, and φ were at their zero positions. The sample position in memDAC was optically adjusted to the instrument centre, defined by the cross point of all diffractometer axes.

Taking into account the relationship between the two reference systems of the IPDS-II and four-circle Eulerian diffractometers, we could deduce an approximate orientation matrix of the single crystal on HEiDi. This facilitated finding the reflections with the point detector. After subsequent centring of these reflections and refinement of the orientation matrix we calculated the offset of the two diffractometers, which results in small deviations in the angular values of χ and φ in the Eulerian geometry of the four-circle diffractometer HEiDi with respect to the angular values deduced from the orientation matrix from IPDS-II. Knowing the exact transformation between both orientation matrices we can now efficiently use the peak search routines in the reciprocal space with the point detector on HEIDI based on the orientation matrices obtained on our laboratory X-ray instrument in future experiments. In a similar way, it is possible to use the orientation matrices from other diffractometers, provided the transformation between the two reference systems is known. The small additional angular deviations can then be straightforwardly determined, leading altogether to a reduction of the measurement time compared to strategies

where the classical search routines are used at HEiDi. These search routines can easily take up to 1 or 2 days of beamtime depending on the size of the crystal.

The software at HEiDi now includes a mathematical model describing the position of memDAC when rotating the sample. With the help of this algorithm, diffracted beams not passing the cell through both diamonds but hitting the body are marked as "shaded" and the corresponding reflections are excluded automatically from the measurement. The routine furthermore checks the possibilities to rotate the sample in DAC around the $\mathbf{H}_{hkl}$ vector and determines whether an alternative ψ position is available where the shading can be avoided and the reflections are accessible.

For the primary neutron optics, a setup with 0.5 mm Er-filter to supress $\lambda/3$ contamination and the adjustable 3 mm BN (boron nitride) pipe collimator were used. For the secondary optics, a 16 mm BC (boron carbide) tube for suppression of scattering from the sample environment and a detector slit of 10*15 mm² (width*height) to minimize background were used. All reflections were measured with ω rocking scans of 10 s/step using a point detector. If significant ($I>3\sigma$), they were remeasured for up to additional 10 s/step in order to increase their accuracy. The combined effect of the diamond seat pinholes and ω scans was that the background due to powder lines originating from the sample environment was minimal. Because of the restrictions in beamtime and in the angular range of DAC, only ($\pm h +k \pm l$) reflections up to $2\theta=65°$ were considered for collection.

Synchrotron single-crystal experiments in memDAC (Table 1) were conducted on the beamline P24 (Chemical Crystallography) at PETRA-III (Hamburg) using a marCCD165 detector on the kappa diffractometer (station EH1, λ = 0.494 Å). The exposure time per frame was 1 second. A filter (a Ni foil with the thickness of 50 μm) was additionally used to attenuate the primary beam. The data were indexed and integrated with the software *CrysAlis* (Oxford Diffraction, 2007). The obtained lattice parameters and unit-cell volume are a = 6.7705(6) Å, c = 4.7044(2) Å, and V = 186.76(4) Å^3, respectively.

Structural refinements

For all structural refinements with the program Jana2006 (Friese *et al*., 2013; Petricek *et al*., 2014), the lattice parameters obtained from the synchrotron data were used due to their higher accuracy. The comparatively high internal R-values for both neutron and synchrotron data can possibly be attributed to effects due to attenuation of the diamonds ("diamond dips", Loveday, 1990). Initially, the refinements of the synchrotron and neutron data were performed separately to test their internal consistency (Tables 1-5). Due to the limited number of reflections available (determined by the opening angle of the cell), the displacement parameters of the atoms were refined isotropically from the neutron data.

A comparison of the atomic coordinates from the present neutron data with the ones obtained earlier (Grzechnik *et al*., 2018) shows that they agree very well within their ESDs (Table 4). The interatomic distances are also identical within their ESDs to those from our *panoramic* cell (Table 5). On the other hand, the completeness of the data in memDAC is significantly lower. The fraction of unique reflections measured out to the angle $\theta_{full,}$ i.e., to the angle at which the measured reflection count is close to be complete, is 62% at θ_{full} = 20.22 for memDAC as compared to 76% at θ_{full} = 39.34° for the *panoramic* cell (Grzechnik *et al*., 2018).

In a second step, a joint refinement combining the synchrotron and neutron data using the available options in the program Jana2006 (Petricek *et al*., 2014) was performed. The corresponding F_{obs}-F_{calc} plots are shown in Figure 2. There are approximately 10 times more reflections measured with the synchrotron radiation than with neutrons. As can be seen from Table 3, the atomic coordinates and displacement parameters in the joint refinement are identical with the ones from the refinement of the synchrotron data alone.

The refinement with the synchrotron data alone showed that it was not possible to refine the Mn and Fe occupancies reliably, due to the limited contrast of these neighbouring elements in X-ray diffraction. To distinguish these two elements, the information from the neutron data is clearly needed. Initially, Mn and Fe were equally distributed on the two available Wyckoff positions *6g* and *4d* (Table 4). The refinement of the occupancies yielded the model, in which the position *6g* is partially occupied by Mn and Fe, while the position *4d* is essentially occupied by Fe. Despite the fact that only relatively limited neutron data are available, a comparison with earlier published structural data based on neutron single-crystal diffraction at ambient (Hering et.al., 2015) and high (Grzechnik et.al., 2018) pressures shows that taking them into account in the refinement still allows to unambiguously refine the occupancies of Mn and Fe on the available sites in agreement with the earlier results (like in the earlier refinements, the sum of occupancies was restricted in such a way that the overall stoichiometry corresponded to the ideal one $MnFe_4Si_3$ in accordance with chemical analysis). It is noteworthy that a test carried out with the present neutron data shows that, even if only the 10 strongest reflections are included, the occupancy factors are still correct and only their standard deviations become slightly higher. This implies that for answering other specific questions, regarding, for instance, magnetic ordering or the positions of hydrogen bonds, a comparatively small number of reflections measured with neutrons would also be sufficient if they are combined with X-ray data.

Conclusions

Our study confirms that it is possible to determine the crystal structure of a compound under high pressure using a combination of neutron and X-ray data measured on the same crystal under identical conditions. The *transmission* cells described in this study can be used on various diffractometers at laboratory X-ray, synchrotron, and neutron facilities.

The major problem in high-pressure investigations using neutron single-crystal diffraction in diamond anvil cells, especially using a point detector, is the elevated time needed to measure a complete dataset due to the small sample volume and the comparatively low flux of the neutron beam. However, in many cases a full neutron dataset does not necessarily have to be measured. Rather small a number of reflections, which are relevant to the scientific question one wants to answer, can be selected to reduce the required beamtime. Complementary data can then be measured with X-ray diffraction, with which the data collection is more efficient.

Currently, the opening angles of our *transmission* DAC are 80°, which is a standard in the diamond anvil cells for single-crystal diffraction. We are now designing new cells made of NiCrAl (Cheng *et al*., 2019) for neutron and X-ray diffraction with a larger opening that would allow a wider access to the reciprocal space, close to the one in our *panoramic* diamond anvil cell (Grzechnik *et al*., 2018). The resulting improvement in the quality and redundancy of the neutron data will mitigate the effect of extinction and radiation attenuation by the diamond anvils. The latter has been treated semi-empirically for time-of-flight neutron diffraction (Guthrie *et al*., 2016). It remains to be accounted for also in monochromatic neutron scattering.

Acknowledgments

The neutron measurements were performed on the single-crystal diffraction beamline HEiDi operated jointly by RWTH Aachen (Institute of Crystallography) and Forschungszentrum Jülich GmbH (JCNS) within the JARA cooperation. Parts of this research were also carried out at PETRA-III. We acknowledge DESY (Hamburg, Germany), a member of the Helmholtz Association HGF, for the provision of experimental facilities.

Funding information

This work was supported by the projects 05K16PA3 (to Georg Roth, Martin Meven, and Andrzej Grzechnik) and 05K19PA2 (to Martin Meven, Vladimir Hutanu, Andrzej Grzechnik, Robert Georgii, and Yixi Su) from the Bundesministerium für Bildung und Forschung (BMBF).

References

Binns, J., Kamenev, K.V., McIntyre, G.J., Moggach, S.A. & Parsons, S. (2016). *IUCrJ*, **3**, 168-179.

Bull, C.L., Guthrie, M., Archer, J., Fernandez-Diaz, M.T., Loveday, J.S., Komatsu, K., Hamidov, H., Nelmes, R.J. (2011). *J. Appl. Cryst*. **44**, 831-838.

Ceretti, M., Wahyudi, O., Gilles, A., Meven, M., Villesuzanne, A. & Paulus, W. (2018). *Inorg. Chem*., **57**, 4657-4666.

Cheng, Y., Brenk, J., Friedrich, B., Perßon, J., Maraytta, N., Gibson, J.S.K.-L., Korte-Kerzel, S., Roth, G., Su, Y., Zhu, F., Paulmann, C. & Grzechnik, A. (2019). *Mater. Sci. Tech*., https://doi.org/10.1080/02670836.2019.1578077.

Devi, P., Singh, S., Dutta, B., Manna, K., D'Souza, S.W., Ikeda, Y., Suard, E., Petricek, V., Simon, P., Werner, P., Chadhov, S., Parkin, S.S.P., Stuart, S.P., Felser, C. & Pandey, D. (2019). *Phys. Rev. B*, **97**, 224102.

Eich, A., Grzechnik, A., Caron, L., Cheng, Y., Wilden, J.S., Deng, H., Hutanu, V., Meven, M., Hanfland, M., Glazyrin, K., Hering, P., Herrmann, M.G., Ait Haddouch, M., Friese, K. (2019). *Mater. Res. Expr*., https://iopscience.iop.org/article/10.1088/2053-1591/ab33b3.

Friese, K., Grzechnik, A., Posse, J.M. & Petricek, V. (2013). *High Pressure Res*., **33**, 196-201.

Gatta, G.D., Rotiroti, N., Cámara, F. & Meven, M. (2018). *Phys. Chem. Minerals*, **445**, 819-829.

Goncharenko, I.N. (2007). *High Pressure Res*., **27**, 183-188.

Grzechnik, A., Meven, M. & Friese, K. (2018). *J. Appl. Cryst*., **51**, 351-356.

Guthrie, M. (2015). *J. Phys.: Condens. Matter*, **27**, 153201.

Guthrie, M, Pruteanu, C.G., Donnelly, M.-E., Molaison, J.J., dos Santos, A.M., Loveday, J.S., Boehler, R. & Tulk, C.A. (2016). *J. Appl. Cryst*., **50**, 76-86.

Hering, P., Friese, K., Voigt, J., Persson, J., Aliouane, N., Grzechnik, A., Senyshyn, A. & Brückel, T. (2015). *Chem. Mater*. **27**, 7128-7136.

Jarzembska, K.N., Ślepokura, K., Kamiński, R., Gutmann, M.J., Dominiak, P.M., Woźniak, K. (2017). *Acta Cryst. B*, **73**, 550-564.

Jin, W., Xiao, Y., Bukowski, Z., Su, Y., Nandi, S., Sazonov, A.P., Meven, M., Zaharko, O., Demirdis, S., Nemkovskiy, K., Schmalzl, K., Tran, L.M., Guguchia, Z., Feng, E., Fu, Z. & Brückel, T. (2016). *Phys. Rev. B*, **94**, 184513.

Klotz, S. (2013). *Techniques in high pressure neutron scattering*. Boca Raton: CRC Press.

Kuhs, W.F., Ahsbahs, H., Londono, D. & Finney, J.L. (1989). *Physica B* **156**&**157**, 684-687.

Kuhs, W.F., Bauer, F.C., Hausmann, R., Ahsbahs, H., Dorwarth, R. & Hölzer, K. (1996). *High Press. Res*. **14**, 341-352.

LeToullec, R., Loubeyre, P., Pinceaux, J.P., Mao, H.K. & Hu, J. (1992). *High Pressure Res*., **6**, 379-388.

Loveday, J.S., McMahon, M. I. & Nelmes, R. J. (1990), J. Appl. Cryst. 23, 392-396.

McMahon, M.I., Nelmes, R.J., Kuhs, W.F., Dorwarth, R., Piltz, R.O. & Tun, Z. (1990). *Nature* **348**, 317-319.

McIntyre, G.J., Mélési, L., Guthrie, M., Tulk, C.A., Xu, J. & Parise, J.B. (2005). *J. Phys.: Condens. Matter* **17**, S3017-S3024.

Merlini, M. & Hanfland, M. (2013). *High Pressure Res*., **33**, 511-522.

Merrill, L. & Bassett, W.A. (1974). *Rev. Sci. Instrum*., **45**, 290-294.

Meven, M. & Sazonov, A. (2015). *J. Large Scale Facilities*, **1**, A7.

Oxford Diffraction (2007). *CrysAlis*. Oxford Diffraction Ltd, Abingdon, Oxfordshire, England.

Petricek, V., Dusek, M. & Palatinus, L. (2014). *Z. Krist*., **229**, 345-352.

Regnat, R., Bauer, A. Senyshyn, A., Meven, M., Hradil, K., Jorba, P., Nemkovski, K., Pedersen, B., Georgii, R., Gottlieb-Schönmeyer, S. & Pfleiderer, C. (2018). *Phys. Rev. Mater.*, **2**, 054413.

Ridley, C.J. & Kamenev, K.V. (2014). *Z. Kristallogr*. **229**, 171-199.

Stoe & Cie (2013). *X-Area.* Stoe & Cie, Darmstadt, Germany.

Truong, K.-N., Merkens, C., Meven, M., Faßbänder, B., Dronskowski, R. & Englert, U. (2017). *Acta Cryst*. B, **73**, 1172-1178.

Truong, K.-N., Meven, M., Englert, U. (2018). *Acta Cryst*. C, **74**, 1635-1640.

Table 1 Experimental single-crystal data on $MnFe_4Si_3$ ($P6_3/mcm$, $Z = 2$) measured with synchrotron and neutron diffraction.

	synchrotron	neutron
Data collection		
No. meas. refl.	509	56
Range of *hkl*	$-10 \le h \le 9$	$0 \le h \le 6$
	$-7 \le k \le 4$	$-3 \le k \le 0$
	$-7 \le l \le 7$	$0 \le l \le 4$
No. obs. refl. †	106	15
$R(int)_{obs}$ ‡	13.10	20.65
Redundancy	4.8	2.6

† Criterion for observed reflections is $|Fobs| > 3\sigma$.
‡ All agreement factors are given in %, weighting scheme is $1/[\sigma^2(Fobs) + (0.01Fobs)^2]$.

Table 2 R-factors overview for the separate refinements of the synchrotron and neutron data.

	synchrotron	neutron
R_{obs}	6.21	7.00
wR_{obs}	7.60	4.41
GoF_{obs}	6.50	1.93
No. pars.	12	7

Table 3 R-factors overview for the joint refinement of the synchrotron and neutron data (the number of refined parameters is 14).

	Block 1 (synchrotron)	Block 2 (neutron)
R_{obs}	6.19	9.70
wR_{obs}	7.58	7.10
GoF_{obs}	6.02	7.74

Table 4 Refined structural parameters for $MnFe_4Si_3$ ($P6_3/mcm$, $Z = 2$) – italics: synchrotron diffraction (a separate refinement); normal fonts: neutron diffraction (a separate refinement); bold fonts: both synchrotron and neutron diffraction (a joint refinement).

Atom	Wyckoff position	Occupancy	*x*	*y*	*z*	U_{eq}
Mn1	*6g*	*0.3333*	*0.7649(3)*	*0.7649(3)*	*0.25*	*0.0150(8)*
		0.33(2)	0.759(3)	0.759(3)	0.25	0.025(9)
		0.32(2)	**0.7649(3)**	**0.7649(3)**	**0.25**	**0.0151(7)**
Fe1		*0.6667*	*0.7649(3)*	*0.7649(3)*	*0.25*	*0.0150(8)*
		0.67(2)	0.759(3)	0.759(3)	0.25	0.025(9)
		0.68(2)	**0.7649(3)**	**0.7649(3)**	**0.25**	**0.0151(7)**
Fe2	*4d*	*1.0*	*0.6667*	*0.3333*	*0*	*0.0132(6)*
		0.99	0.6667	0.3333	0	0.025(8)
		0.98	**0.6667**	**0.3333**	**0**	**0.0132(6)**
Mn2		*0.0*	*0.6667*	*0.3333*	*0*	*0.0132(6)*
		0.01	0.6667	0.3333	0	0.025(8)
		0.02	**0.6667**	**0.3333**	**0**	**0.0132(6)**
Si	*6g*	*1.0*	*0.3998(4)*	*0.3998(4)*	*0.25*	*0.013(1)*
		1.0	0.391(6)	0.391(6)	0.25	0.028(8)
		1.0	**0.3998(5)**	**0.3998(5)**	**0.25**	**0.013(1)**

Atom	U_{11}	U_{22}	U_{33}	U_{12}	U_{13}	U_{23}
Mn1/Fe1	*0.016(1)*	*0.010(1)*	*0.017(1)*	*0.0051(6)*	*0*	*0*
	0.016(1)	**0.10(1)**	**0.017(8)**	**0.0051(5)**	**0**	**0**
Fe2	*0.013(1)*	*0.013(1)*	*0.013(1)*	*0.0066(6)*	*0*	*0*
	0.013(1)	**0.013(1)**	**0.013(1)**	**0.0066(5)**	**0**	**0**
Si	*0.012(2)*	*0.010(2)*	*0.017(1)*	*0.0049(9)*	*0*	*0*
	0.012(1)	**0.010(2)**	**0.017(1)**	**0.0050(8)**	**0**	**0**

Table 5 Selected interatomic distances (in Å) in $MnFe_4Si_3$.

		synchrotron	neutron	synchrotron & neutron
Mn1-Mn1	2x	2.757(3)	2.83(3)	2.757(2)
Mn1-Mn1	4x	2.840(1)	2.863(9)	2.840(1)
Mn1-Fe2	4x	2.902(2)	2.88(1)	2.902(3)
Mn1-Si		2.472(4)	2.49(4)	2.472(4)
Mn1-Si	2x	2.356(3)	2.32(3)	2.356(3)
Mn1-Si	2x	2.603(2)	2.56(2)	2.603(2)
Fe2-Fe2	2x	2.3522(2)	2.3522(2)	2.3522(2)
Fe2-Si	6x	2.380(3)	2.40(4)	2.380(3)
Si-Si	2x	2.715(2)	2.77(3)	2.715(3)

Figure captions

Figure 1 The cell used in this study – (a) a schematic cross-section and different views with and without the membrane and cup (the valve is not shown), (b) the cell mounted on the laboratory X-ray diffractometer IPDS-II, (c) the cell mounted on the four-circle diffractometer at HEiDi.

Figure 2 Observed (F_{obs}) versus calculated (F_{calc}) structure factors based on symmetry independent reflections from a joint refinement of the synchrotron and neutron data.

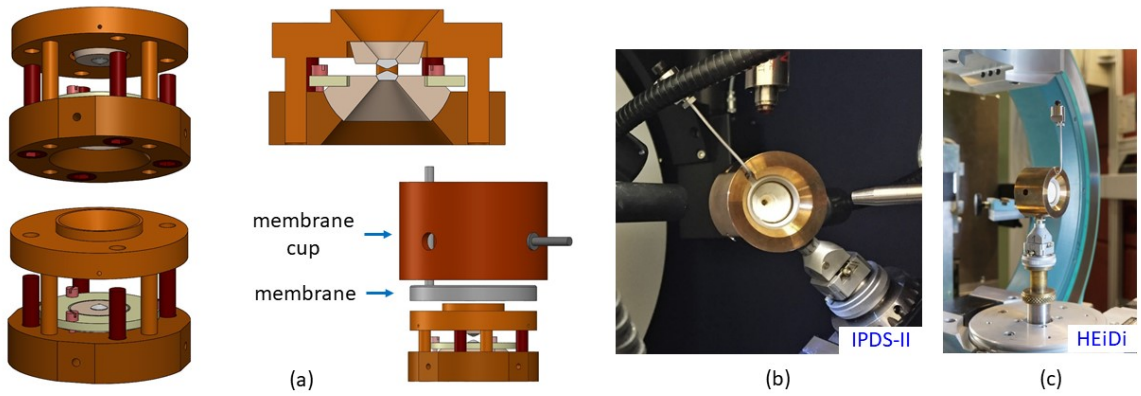

(a) (b) (c)

Figure 1.

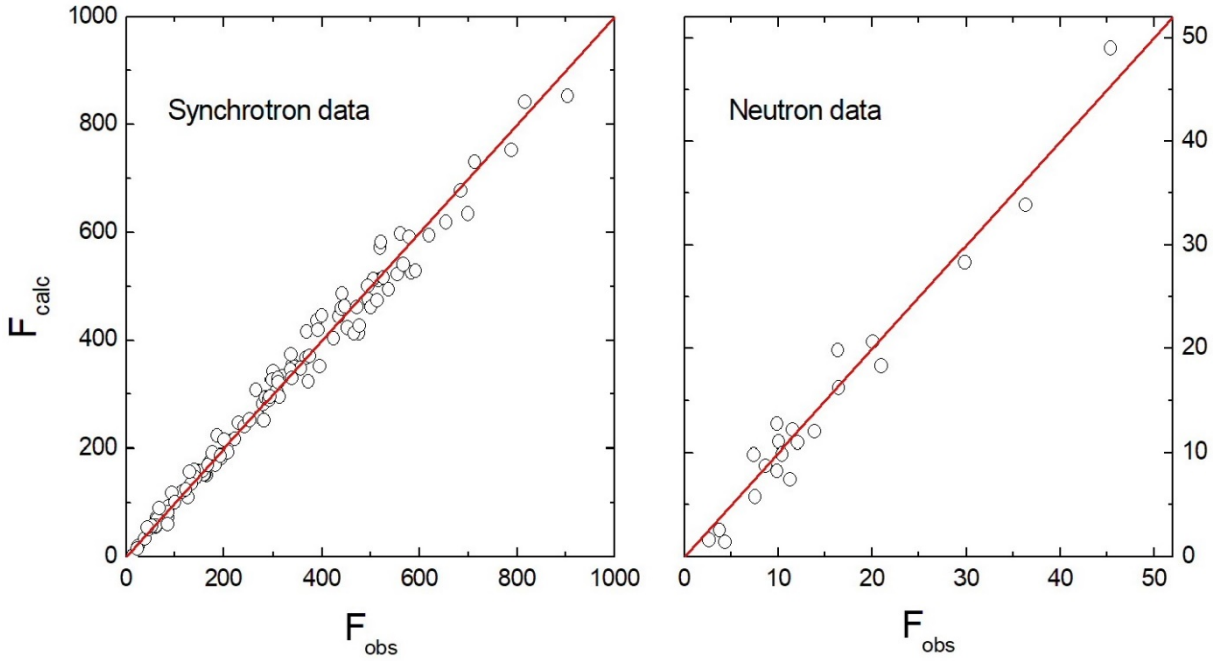
Synchrotron data
Neutron data
F calc
F obs
F obs
0
200
400
600
800
1000
0
10
20
30
40
50

Figure 2.